NASA TM X-161

NASA TM X-161

TECHNICAL MEMORANDUM X-161

EFFECTS OF STING-SUPPORT INTERFERENCE ON THE BASE PRESSURES OF A MODEL HAVING A BLUNT-NOSED CYLINDER BODY AND A CONICAL FLARE AT MACH NUMBERS OF 0.65 TO 2.20

By David E. Reese, Jr., and William R. Wehrend, Jr.

Ames Research Center
Moffett Field, Calif.

NATIONAL AERONAUTICS AND SPACE ADMINISTRATION
WASHINGTON
February 1960

DATE SENT	ISSUED TO
4/28/60	Hill W. FM
1-30-62	Erickson S,D
12-29-64	D. Stuvie - VAB
9/27/65	V. PETERSON - HAB

LIBRARY CIRCULATION SLIP
GPO 978103

DATE PROMPTED
Q
62
64
65

the base pres-
linder body and
to 2,20 Reese
Wehrend

16—0901

NATIONAL AERONAUTICS AND SPACE ADMINISTRATION

TECHNICAL MEMORANDUM X-161

EFFECTS OF STING-SUPPORT INTERFERENCE ON THE BASE PRESSURES OF A MODEL HAVING A BLUNT-NOSED CYLINDER BODY AND A CONICAL FLARE AT MACH NUMBERS OF 0.65 TO 2.20*

By David E. Reese, Jr., and William R. Wehrend, Jr.

SUMMARY

A wind-tunnel investigation was conducted to determine the effects of sting-support interference on the pressures at the base of a model incorporating a blunt-nosed cylinder body and a conically flared afterbody. The support consisted of a cylindrical sting followed by a sting flare terminating in a cylindrical support. Various sting lengths and diameters were investigated over a Mach number range from $M = 0.65$ to 2.20 and at angles of attack from 0° to 18°. The Reynolds number (based on body diameter) varied from a maximum of 1.1×10^{6} at $M = 1.10$ to a minimum of 0.5×10^{6} at $M = 2.20$.

The results of the investigation showed that the critical value of the ratio of sting length to model-base diameter was greater than 4.80 at subsonic and transonic speeds and less than 2.55 at supersonic speeds. Angle of attack had negligible effect on the critical sting length. The pressures at the model base were affected by changes in sting diameter at all Mach numbers investigated. For the sting diameters considered, an increase in sting diameter made the pressure coefficient at the base more negative, this effect being greatest at $M = 1.00$.

INTRODUCTION

The need for a complete understanding of the effects of model-support interference on wind-tunnel test results has long been recognized. The requirements for a minimum-interference sting-support system for an ogive-cylinder body with and without a boattail with turbulent boundary layer at Mach numbers from 0.60 to 1.40 have been considered in reference 1. However, for wind-tunnel investigations of shapes incorporating a flared afterbody to provide stability, the interference problem must be re-evaluated to insure minimum-interference sting support systems. The present investigation was undertaken to provide information on a model incorporating a blunt-nosed cylinder and a conically flared afterbody. The Mach number range of this study was from 0.65 to 2.20.

*Title, Unclassified

Although reference 1 had shown an effect of support interference on both the foredrag and on the base drag (i.e., base pressure) of a model with boattailing, the interference effect of the support on the base drag was the more severe. Further, the results indicated no effect of support interference on the foredrag of a model with cylindrical afterbody. Therefore, it was considered adequate to confine the present study to the effects of support interference on the model base pressures. The effects of changes of either sting diameter or sting length as well as the effect of the base diameter of the conically flared afterbody of the model on the support interference were investigated.

NOTATION

C_p base pressure coefficient, $\frac{p - p_\infty}{q_\infty}$

d diameter of sting, in.

D diameter of model base, in.

f length of model flare, in.

l length of sting of constant diameter between model base and sting flare, in.

m length of model, in.

M Mach number

p static pressure

q dynamic pressure

R Reynolds number

x longitudinal station measured from model nose

α angle of attack relative to model axis of symmetry, deg

α_n nominal angle of attack

Subscripts

∞ free stream

av average value

APPARATUS AND TESTS

The investigation was conducted in the Ames 6- by 6-foot supersonic wind tunnel, which is a closed-circuit, variable-pressure type with a Mach number range continuous from approximately 0.65 to 2.30. The floor and ceiling of the test section are perforated to permit testing at transonic speeds.

Geometric characteristics of the models and sting supports investigated are shown in figure 1. Two models differing only in flare length were tested. The nose for both configurations was elliptical with the ratio of minor to major axis of 0.50, and the minor axis alined with the longitudinal axis of the body. A photograph of the model with the shorter flare installed on the sting of smallest diameter is shown in figure 2. The models were constructed of polished steel while the stings were made of Fiberglas around a steel core. To increase the sting diameter, Fiberglas sleeves were merely slipped over the basic sting. The stings were sanded smooth and painted. As shown in figure 1 three sting lengths, three sting diameters, and two model-base configurations were investigated.

It should be noted that the model-base location in the wind tunnel was fixed for this investigation to preclude possible influence of any longitudinal pressure gradients in the tunnel. To test shortened stings, dummy sting flares were installed ahead of the sting flare of the model support system.

Pressure measurements were made at 12 orifices in the model base as shown in figure 3. The pressure readings were photographically recorded from a liquid tube manometer (tetrobromoethane fluid) for later reduction and computation. Data were obtained at nominal angles of attack of 0°, 6°, 12°, and 18° at Mach numbers from 0.65 to 2.20. The variation of Reynolds number (based on the model body diameter of 3.040 in.) with Mach number is shown in figure 4.

ACCURACY OF DATA

The accuracy of the data was determined by the least count reading of the various instruments involved. In addition, at $M = 1.00$, the free-stream static pressure in the wind tunnel showed small fluctuations around the mean static pressure as a result of some unsteadiness in the flow. This affected the accuracy with which both Mach number and base pressure could be measured. On the basis of these factors the accuracy of the data was determined to be:

M	± 0.010
α	± 0.100
C_p	± 0.006

It should be noted that in certain instances in the tabulated data, particularly at Mach numbers of 1.60 and 2.20, the pressure coefficients indicated for orifices 2 and 10 were in error. These erroneous readings were caused by excessive lag introduced as a result of outside equipment in parallel with these particular orifice systems for monitoring purposes. As indicated in table I these questionable readings were not included in the computation of the average pressure coefficient.

RESULTS AND DISCUSSION

The aerodynamic interference caused by a sting-type model support in wind-tunnel experimentation has been shown in references 1 and 2 to result from two causes: the interference to the flow resulting from the proximity of the sting flare, "the length effect," and the interference resulting from the presence of the constant-diameter sting, "the diameter effect." Before considering these effects in the light of the results of the present investigation, it might be well to consider first the distribution of pressure over the model base.

Distribution of Pressure Over the Model Base

All of the results obtained in the present investigation are presented in table I. Typical results for model configuration 1 (see fig. 1) have been plotted in figure 5 to show the distribution of pressure over the model base. In this figure the pressure coefficient is plotted as a radial distance from the origin at the angular displacement corresponding to the relative angular position of the particular pressure orifice on the model base. In addition a circle is shown of radius equal to the average of the pressure coefficients indicated by all the pressure orifices. It is interesting to note that for a Mach number of 0.65, the change in base pressure with angle of attack is not uniform over the surface of the base. Starting with uniform pressure at zero angle of attack, an increase in angle of attack causes an increase in the magnitude of the base pressure coefficient, but the increase is faster at the top of the model than at the bottom. However, at 18° the pressure distribution is again uniform. The nonuniform variation of pressure distribution is most pronounced at subsonic Mach numbers and disappears at a Mach number of 2.20. In all cases the variation is small so that in the ensuing discussion of sting geometry effects only the average pressure coefficients will be used.

Effect of Sting Length

The effects of sting length on the model base-pressure coefficients for a ratio of sting diameter to model-base diameter of 0.451 are shown in figure 6 for various Mach numbers and model angles of attack. The point of interest here is the critical sting-length to base-diameter ratio, defined as the minimum l/D required to obtain the same average pressure coefficient at the model base as would be obtained with a sting of infinite length. It can be seen that at Mach numbers of 1.30 and above, this critical sting-length ratio is smaller than 2.55, the value for the shortest sting tested in this investigation. At Mach numbers below 1.30, the critical l/D appears to be somewhat larger than 4.80, the value corresponding to the longest sting tested, particularly at a Mach number of 1.00. From a comparison of these results with those of reference 1 which show critical values of l/D of approximately 2.60 at $M = 1.40$ and 4.00 at $M = 1.00$ or 0.60 for a model with cylindrical afterbody, it appears that the flared afterbody caused an increase of critical l/D at subsonic and transonic speeds but not at supersonic speeds.

Using potential theory, Tunnell has developed an expression for the effect of sting length on the pressure at the position of the base which is valid for the subsonic speed range (ref. 2). The theoretical curve has been plotted in figure 6. It is seen that the theory predicts the variation of base pressure with l/D fairly well. As was mentioned in reference 2, agreement in the magnitude of the theoretical and experimental pressures is not to be expected since the theory does not take into account the presence of the model.

Variation of angle of attack appears to have negligible effect on the critical l/D. As shown by figure 6, the interference effect caused by a sting of less than critical l/D is to decrease the negative pressure coefficient at the model base.

Effect of Sting Diameter

The effects of sting diameter on the model base pressure coefficients for ratios of sting length to model-base diameter of 4.80 and 4.31 are shown in figure 7 for various Mach numbers and model angles of attack. (It will be noted that the data for $l/D = 4.31$ were obtained with the model with the larger flare (fig. 1).) From these data it is not possible to determine a critical sting diameter to model-base diameter ratio, defined as the maximum d/D for obtaining the same average pressure coefficient at the model base as would be obtained with a sting of "zero" diameter. However, for the d/D ratios considered, the effect of increasing the sting diameter is to increase the negative pressure

coefficient at all Mach numbers, the magnitude of the effect being greatest at angle of attack near zero and more pronounced at Mach numbers near unity. The increase of pressure coefficient with increase of d/D is in agreement with the trends indicated in reference 1 for d/D ratios greater than 0.25 for a model with no boattailing. It should be noted, however, that reference 1 indicates an initial decrease of pressure coefficient with the addition of a sting of finite diameter for a cylindrical model. No attempt was made to confirm this effect in the present investigation.

Also shown in figure 7 is the effect of the larger flare. The points obtained with the larger flare are denoted by flagged symbols. It can be seen that the increase in flare base diameter had a negligible effect on the sting-diameter interference.

CONCLUSIONS

The results of the investigation to determine the effects of changes of sting length and sting diameter on the base pressures of a model incorporating a blunt-nosed cylinder body and a conically flared afterbody revealed the following results:

1. The critical value of the ratio of sting length to model-base diameter, l/D, was greater than 4.80 at subsonic and transonic speeds and less than 2.55 at supersonic speeds.

2. The effect of a sting shorter than the critical l/D was to decrease the negative pressure coefficient at the base of the model.

3. Angle-of-attack changes had negligible effect on the critical sting-length to model-base diameter ratio.

4. The pressures at the model base were affected by changes in the ratio of sting diameter to model-base diameter for all sting diameters and all Mach numbers tested. For the sting diameters considered, an increase in sting diameter made the pressure coefficient at the base more negative, this effect being greatest at a Mach number of 1.00.

Ames Research Center
National Aeronautics and Space Administration
Moffett Field, Calif., July 9, 1959

REFERENCES

1. Lee, George, and Summers, James L.: Effects of Sting-Support Interference on the Drag of an Ogive-Cylinder Body With and Without a Boattail at 0.6 to 1.4 Mach Number. NACA RM A57I09, 1957.

2. Tunnell, Phillips J.: An Investigation of Sting-Support Interference on Base Pressure and Forebody Chord Force at Mach Numbers From 0.60 to 1.30. NACA RM A54K16a, 1955.

TABLE I.- TABULATED TEST RESULTS

(a) Model configuration 1

M	α, deg	C_p at orifice												$C_{p_{av}}$
		1	2	3	4	5	6	7	8	9	10	11	12	
0.65	-0.06	0.291	0.296	0.298	0.284	0.272	0.272	0.281	0.293	0.295	0.301	0.304	0.304	0.291
	6.13	.300	.302	.304	.330	.368	.383	.381	.382	.361	.366	.372	.328	.348
	12.37	.360	.363	.365	.375	.398	.407	.407	.405	.386	.390	.395	.368	.385
	18.60	.417	.419	.421	.415	.425	.436	.439	.436	.420	.423	.426	.417	.425
.80	-.05	.292	.297	.295	.284	.278	.284	.294	.299	.301	.307	.305	.303	.295
	6.23	.328	.329	.331	.357	.392	.403	.399	.403	.384	.388	.394	.353	.372
	12.57	.391	.395	.397	.404	.424	.429	.429	.429	.424	.425	.425	.403	.415
	18.57	.439	.443	.444	.444	.454	.463	.464	.462	.452	.456	.458	.446	.452
1.00	.21	.385	.395	.387	.384	.386	.389	.390	.386	.384	.394	.385	.388	.388
	6.68	.493	.483	.490	.502	.522	.531	.527	.528	.518	.513	.523	.501	.511
	13.14	.569	.576	.571	.574	.583	.589	.588	.588	.582	.590	.586	.575	.581
	19.48	.592	.592	.595	.593	.597	.599	.600	.599	.595	.595	.599	.594	.596
1.30	.15	.332	.331	.335	.327	.326	.330	.330	.330	.332	.332	.334	.338	.331
	6.47	.337	.338	.340	.347	.362	.367	.366	.365	.353	.353	.358	.346	.353
	13.01	.396	.392	.398	.400	.407	.409	.409	.408	.404	.399	.406	.398	.402
	18.25	.444	.444	.445	.445	.446	.446	.446	.444	.439	.440	.443	.441	.444
1.60	0	.263	[a].260	.266	.263	.250	.244	.252	.250	.250	[a].247	.250	.263	.255
	6.31	.260	[a].262	.264	.262	.272	.275	.278	.275	.266	[a].261	.268	.265	.268
	12.67	.303	[a].290	.303	.307	.310	.312	.312	.312	.309	[a].295	.312	.306	.309
	18.97	.348	[a].333	.348	.350	.353	.349	.349	.347	.352	[a].334	.353	.349	.350
2.20	.68	.121	[a].077	.119	.122	.128	.127	.122	.122	.122	[a].072	.125	.119	.123
	6.87	.149	[a].117	.146	.149	.154	.154	.152	.150	.149	[a].111	.151	.147	.150
	13.08	.174	[a].146	.173	.174	.177	.177	.177	.177	.174	[a].145	.177	.174	.175
	19.25	.191	[a].164	.189	.191	.194	.193	.190	.193	.191	[a].161	.193	.190	.191

(b) Model configuration 2

M	α, deg	C_p at orifice												$C_{p_{av}}$
		1	2	3	4	5	6	7	8	9	10	11	12	
0.65	-0.11	0.306	0.307	0.309	0.302	0.296	0.294	0.296	0.300	0.302	0.302	0.307	0.309	0.303
	6.03	.320	.320	.322	.322	.361	.390	.390	.390	.355	.359	.364	.323	.351
	12.13	.388	.390	.390	.378	.386	.412	.412	.412	.376	.382	.384	.382	.391
	18.27	.429	.432	.436	.429	.423	.442	.440	.440	.412	.421	.425	.437	.431
.80	-.05	.324	.327	.327	.326	.325	.318	.308	.301	.312	.317	.315	.321	.318
	6.09	.334	.334	.335	.345	.387	.408	.408	.408	.379	.381	.387	.343	.371
	12.29	.410	.410	.413	.403	.424	.436	.434	.435	.409	.411	.418	.406	.417
	18.44	.461	.461	.462	.458	.464	.477	.476	.476	.451	.454	.461	.463	.464
1.00	.27	.416	.424	.419	.416	.416	.417	.417	.417	.413	.422	.417	.417	.418
	6.48	.479	.479	.478	.501	.542	.554	.554	.552	.531	.533	.537	.493	.519
	12.74	.560	.555	.562	.558	.576	.585	.583	.583	.569	.565	.574	.558	.569
	19.00	.642	.648	.642	.640	.641	.645	.645	.645	.637	.648	.643	.643	.643
1.30	.15	.357	.354	.357	.355	.356	.352	.356	.357	.356	.351	.356	.358	.355
	6.34	.365	.365	.368	.355	.366	.389	.386	.387	.362	.357	.361	.362	.369
	12.58	.407	.402	.407	.402	.411	.413	.412	.414	.409	.402	.411	.403	.408
	18.78	.462	.455	.462	.459	.464	.464	.462	.462	.459	.451	.461	.461	.460
1.60	0	.281	.280	.280	.276	.279	.275	.275	.276	.276	.274	.274	.282	.277
	6.16	.286	.285	.287	.284	.278	.282	.282	.283	.279	.277	.277	.284	.282
	12.36	.317	.300	.317	.313	.317	.317	.310	.317	.315	.303	.317	.316	.314
2.20	.68	.126	[a].085	.123	.127	.133	.129	.125	.128	.128	[a].080	.129	.124	.127
	6.77	.158	[a].122	.155	.160	.160	.160	.155	.157	.156	[a].117	.156	.156	.157
	12.94	.173	[a].147	.173	.175	.174	.174	.169	.173	.171	[a].138	.172	.173	.173
	18.96	.193	[a].167	.191	.194	.194	.193	.189	.191	.190	[a].163	.193	.191	.191

[a]Value not used in computing average C_p.

TABLE I.- TABULATED TEST RESULTS - Continued

(c) Model configuration 3

M	α, deg	C_p at orifice												$C_{p_{av}}$
		1	2	3	4	5	6	7	8	9	10	11	12	
0.65	-0.11	0.339	0.342	0.344	0.335	0.326	0.326	0.326	0.327	0.335	0.335	0.340	0.343	0.335
	5.99	.348	.350	.350	.335	.357	.395	.392	.395	.355	.359	.365	.340	.362
	12.08	.398	.397	.400	.401	.375	.415	.410	.410	.362	.365	.377	.412	.394
	18.23	.454	.456	.459	.468	.418	.446	.442	.442	.412	.422	.431	.476	.444
.80	-.10	.344	.346	.349	.339	.339	.331	.324	.324	.332	.334	.338	.344	.337
	6.03	.359	.359	.360	.350	.386	.427	.421	.428	.386	.389	.398	.352	.385
	12.15	.418	.418	.420	.414	.419	.455	.448	.453	.408	.413	.420	.422	.426
	18.23	.472	.472	.475	.478	.461	.488	.486	.484	.447	.453	.462	.487	.472
1.00	.27	.448	.447	.453	.450	.446	.451	.451	.454	.450	.448	.454	.451	.450
	6.38	.508	.504	.509	.503	.526	.581	.576	.583	.545	.534	.558	.501	.536
	12.54	.582	.580	.583	.573	.583	.615	.611	.615	.580	.580	.588	.580	.589
	18.69	.650	.658	.656	.657	.639	.653	.653	.653	.636	.648	.644	.661	.651
1.30	.15	.404	.402	.406	.403	.389	.401	.403	.404	.403	.401	.405	.404	.402
	6.25	.413	.411	.416	.414	.382	.414	.422	.423	.378	.382	.382	.415	.404
	12.40	.439	.437	.442	.441	.415	.438	.430	.440	.421	.416	.427	.446	.433
	18.50	.468	.465	.469	.470	.449	.462	.462	.466	.458	.454	.461	.470	.463
1.60	0	.306	[a].294	.306	.305	.276	.304	.303	.304	.304	[a].289	.303	.305	.302
	6.08	.313	[a].311	.315	.314	.294	.305	.303	.305	.302	[a].302	.300	.316	.307
	12.21	.335	[a].327	.336	.335	.306	.330	.310	.328	.319	[a].310	.323	.335	.325
	18.29	.374	[a].360	.369	.373	.343	.369	.351	.367	.365	[a].347	.368	.372	.365
2.20	.72	.140	[a].102	.137	.141	.080	.143	.138	.141	.141	[a].096	.143	.138	.134
	6.69	.170	[a].140	.168	.171	.112	.169	.167	.169	.169	[a].134	.169	.169	.163
	12.84	.184	[a].160	.184	.184	.128	.181	.177	.179	.179	[a].150	.179	.184	.176
	18.85	.207	[a].186	.205	.206	.159	.201	.196	.203	.203	[a].181	.202	.202	.198

(d) Model configuration 4

M	α, deg	C_p at orifice												$C_{p_{av}}$
		1	2	3	4	5	6	7	8	9	10	11	12	
0.65	-0.06	0.299	0.299	0.303	0.288	0.288	0.288	0.288	0.299	0.307	0.307	0.311	0.309	0.299
	6.02	.310	.313	.313	.311	.345	.376	.375	.375	.344	.351	.353	.314	.340
	12.20	.377	.377	.379	.369	.377	.403	.401	.401	.368	.371	.375	.370	.381
	18.23	.423	.426	.430	.425	.418	.439	.439	.439	.412	.418	.421	.426	.426
.80	-.10	.315	.316	.318	.304	.295	.288	.297	.315	.323	.327	.327	.327	.313
	6.13	.317	.312	.317	.326	.368	.391	.391	.391	.360	.360	.369	.324	.352
	12.25	.398	.400	.400	.393	.408	.427	.422	.424	.400	.405	.408	.394	.407
	18.36	.457	.458	.458	.456	.457	.475	.474	.474	.455	.460	.462	.454	.462
1.00	.21	.355	.352	.359	.356	.358	.358	.358	.358	.354	.351	.357	.356	.356
	6.45	.441	.436	.438	.461	.501	.512	.514	.511	.490	.478	.498	.455	.478
	12.67	.547	.551	.549	.545	.562	.571	.571	.571	.555	.563	.560	.545	.558
	18.91	.609	.611	.610	.609	.609	.613	.614	.614	.606	.612	.611	.610	.611
1.30	.10	.357	.355	.357	.357	.357	.355	.356	.358	.357	.353	.356	.359	.356
	6.36	.369	.367	.370	.357	.368	.391	.388	.390	.362	.362	.365	.367	.371
	12.53	.408	.403	.407	.402	.412	.415	.413	.414	.408	.403	.411	.405	.408
	18.69	.462	.454	.462	.461	.465	.465	.461	.463	.461	.452	.463	.461	.461
1.60	0	.281	.276	.278	.278	.278	.275	.273	.275	.275	.270	.274	.281	.276
	6.13	.288	.285	.288	.284	.280	.284	.284	.286	.279	.278	.278	.286	.283
	12.32	.314	.306	.315	.311	.315	.315	.309	.316	.313	.301	.314	.313	.312
2.20	.69	.115	[a].076	.113	.118	.122	.120	.117	.120	.120	[a].071	.123	.113	.119
	6.75	.154	[a].121	.153	.158	.158	.158	.154	.154	.153	[a].115	.155	.155	.154
	12.90	.174	[a].144	.171	.174	.174	.174	.170	.171	.171	[a].137	.170	.173	.172
	18.92	.190	[a].165	.192	.193	.193	.193	.188	.190	.190	[a].156	.191	.191	.191

[a]Value not used in computing average C_p.

TABLE I.- TABULATED TEST RESULTS - Continued

(e) Model configuration 5

M	α, deg	C_p at orifice												$C_{p_{av}}$
		1	2	3	4	5	6	7	8	9	10	11	12	
0.65	-0.06	0.273	0.277	0.278	0.278	0.278	0.276	0.276	0.279	0.279	0.280	0.282	0.276	0.278
	6.02	.292	.295	.296	.295	.328	.356	.354	.355	.321	.327	.329	.293	.320
	12.15	.359	.360	.364	.352	.356	.386	.382	.383	.347	.352	.357	.353	.363
	18.22	.405	.409	.413	.408	.400	.421	.420	.418	.393	.398	.402	.409	.408
.80	-.10	.274	.275	.277	.276	.277	.279	.280	.284	.281	.288	.285	.279	.280
	6.07	.297	.294	.298	.307	.349	.370	.371	.369	.340	.344	.348	.305	.333
	12.24	.370	.370	.373	.363	.376	.396	.392	.396	.370	.373	.378	.363	.377
	18.36	.421	.421	.421	.421	.421	.447	.447	.447	.422	.424	.424	.424	.428
1.00	.21	.233	.229	.236	.233	.235	.235	.235	.234	.230	.226	.235	.231	.233
	6.44	.335	.342	.333	.356	.397	.409	.410	.408	.386	.399	.393	.350	.377
	12.72	.442	.438	.447	.445	.462	.470	.468	.471	.453	.448	.459	.443	.454
	18.84	.503	.501	.505	.501	.502	.508	.511	.506	.495	.495	.502	.502	.503
1.30	.15	.359	.355	.359	.357	.357	.353	.355	.357	.355	.349	.355	.357	.356
	6.31	.366	.364	.369	.354	.365	.388	.386	.388	.359	.356	.362	.364	.368
	12.57	.407	.401	.408	.400	.412	.414	.412	.415	.408	.400	.411	.403	.408
	18.68	.460	.450	.460	.458	.463	.463	.460	.461	.458	.449	.462	.459	.459
1.60	0	.276	.260	.274	.272	.271	.268	.268	.269	.268	.251	.266	.273	.268
	6.13	.284	.280	.287	.281	.278	.281	.281	.282	.276	.271	.274	.282	.280
	12.31	.313	.303	.315	.309	.314	.314	.306	.315	.310	.298	.313	.311	.310
	18.49	.356	.343	.355	.355	.354	.354	.354	.354	.354	.339	.357	.357	.353
2.20	-0.28	.138	[a].097	.134	.138	.141	.141	.138	.139	.136	[a].089	.138	.133	.137
	6.76	.163	[a].131	.159	.163	.161	.163	.160	.163	.157	[a].124	.157	.161	.161
	12.87	.184	[a].162	.184	.186	.181	.184	.178	.183	.178	[a].155	.180	.183	.182
	18.94	.197	[a].176	.195	.199	.197	.197	.192	.196	.193	[a].169	.193	.195	.196

(f) Model configuration 6

M	α, deg	C_p at orifice												$C_{p_{av}}$
		1	2	3	4	5	6	7	8	9	10	11	12	
0.65	-0.06	0.304	0.305	0.308	0.293	0.287	0.287	0.298	0.306	0.312	0.314	0.314	0.314	0.304
	6.16	.304	.306	.311	.332	.370	.387	.383	.387	.368	.371	.373	.333	.352
	12.42	.358	.361	.363	.372	.395	.409	.409	.407	.391	.394	.397	.371	.386
	18.63	.409	.412	.415	.412	.420	.430	.437	.433	.422	.425	.427	.413	.421
.80	-.05	.303	.303	.304	.292	.286	.294	.305	.314	.316	.317	.319	.315	.306
	6.27	.339	.342	.346	.366	.400	.411	.409	.413	.396	.402	.402	.366	.383
	12.63	.391	.392	.397	.403	.419	.419	.419	.419	.417	.417	.421	.401	.410
	18.94	.442	.446	.447	.445	.453	.459	.463	.460	.451	.455	.457	.447	.452
1.00	.21	.388	.390	.385	.381	.396	.417	.426	.425	.414	.419	.414	.404	.405
	6.74	.496	.493	.495	.511	.535	.541	.538	.540	.527	.529	.531	.506	.520
	13.28	.564	.564	.566	.569	.578	.582	.582	.582	.576	.578	.580	.569	.574
	19.71	.588	.583	.589	.588	.591	.593	.593	.592	.588	.587	.592	.589	.589
1.30	.15	.335	.333	.335	.326	.329	.337	.339	.339	.341	.338	.342	.343	.336
	6.58	.343	.342	.345	.348	.361	.370	.368	.369	.359	.358	.362	.349	.356
	13.06	.390	.386	.393	.393	.398	.401	.400	.401	.396	.393	.400	.393	.395
	19.11	.440	.434	.440	.440	.441	.441	.442	.440	.438	.432	.441	.439	.439
1.60	0	.268	.266	.270	.260	.250	.256	.259	.253	.260	.258	.261	.270	.261
	6.35	.263	.263	.264	.266	.277	.280	.279	.275	.268	.266	.270	.268	.270
	12.76	.313	.310	.313	.313	.315	.317	.318	.317	.315	.313	.316	.314	.315
	19.11	.346	.333	.346	.346	.349	.346	.346	.343	.346	.334	.348	.346	.344
2.20	.68	.115	[a].069	.115	.116	.122	.122	.117	.117	.115	[a].065	.119	.113	.117
	6.88	.147	[a].115	.146	.149	.153	.155	.151	.151	.147	[a].111	.154	.146	.150
	13.10	.168	[a].141	.166	.168	.172	.172	.169	.170	.168	[a].135	.171	.168	.169
	19.35	.190	[a].164	.189	.191	.194	.191	.188	.189	.189	[a].161	.191	.188	.190

[a]Value not used in computing average C_p.

TABLE I.- TABULATED TEST RESULTS - Concluded

(g) Model configuration 7

M	α, deg	C_p at orifice												$C_{p_{av}}$
		1	2	3	4	5	6	7	8	9	10	11	12	
0.65	-0.06	0.302	0.302	0.307	0.300	0.298	0.302	0.307	0.309	0.308	0.310	0.313	0.309	0.306
	6.05	.322	.322	.323	.325	.358	.383	.382	.382	.349	.352	.357	.325	.348
	12.26	.384	.386	.386	.379	.379	.403	.403	.403	.373	.378	.380	.382	.386
	18.32	.425	.428	.431	.428	.417	.431	.434	.431	.413	.417	.420	.431	.426
.80	-.10	.318	.321	.321	.318	.321	.325	.329	.325	.319	.323	.323	.320	.322
	6.11	.335	.335	.337	.346	.382	.401	.400	.400	.376	.379	.382	.345	.368
	12.32	.405	.404	.404	.400	.404	.424	.420	.424	.400	.402	.408	.402	.408
	18.49	.451	.452	.452	.453	.448	.461	.461	.462	.445	.450	.453	.450	.453
1.00	.21	.429	.428	.432	.428	.428	.430	.429	.429	.427	.427	.431	.430	.429
	6.52	.475	.478	.474	.495	.531	.543	.542	.542	.520	.524	.522	.487	.511
	12.81	.582	.579	.584	.583	.593	.601	.600	.601	.586	.587	.592	.582	.589
	19.07	.608	.604	.608	.609	.609	.612	.612	.612	.605	.602	.609	.610	.608
1.30	.15	.360	.355	.359	.352	.356	.354	.355	.357	.355	.349	.354	.358	.355
	6.37	.373	.371	.374	.364	.367	.390	.388	.388	.360	.359	.364	.369	.372
	12.64	.405	.401	.405	.405	.406	.410	.407	.410	.403	.398	.406	.405	.405
	18.92	.459	.453	.459	.459	.460	.460	.458	.459	.457	.451	.459	.460	.458
1.60	0	.280	.282	.279	.274	.274	.271	.270	.271	.272	.272	.271	.279	.275
	6.18	.290	.289	.292	.284	.279	.284	.284	.285	.277	.277	.275	.292	.284
	12.42	.317	.310	.318	.314	.315	.315	.308	.315	.314	.303	.316	.317	.314
	18.60	.360	.344	.357	.357	.358	.358	.353	.357	.357	.340	.359	.357	.355
2.20	.69	.142	[a].105	.138	.141	.145	.145	.142	.142	.142	[a].100	.144	.141	.141
	6.80	.164	[a].134	.161	.161	.159	.162	.160	.160	.160	[a].125	.158	.163	.161
	12.95	.178	[a].153	.177	.177	.175	.175	.173	.175	.174	[a].145	.175	.177	.175
	19.06	.196	[a].173	.193	.196	.196	.195	.191	.194	.193	[a].166	.195	.194	.194

(h) Model configuration 8

M	α, deg	C_p at orifice												$C_{p_{av}}$
		1	2	3	4	5	6	7	8	9	10	11	12	
0.65	-0.06	0.335	0.338	0.341	0.333	0.331	0.328	0.328	0.334	0.333	0.339	0.339	0.341	0.335
	5.99	.348	.347	.351	.338	.354	.388	.384	.387	.351	.355	.361	.345	.359
	12.10	.395	.394	.396	.398	.372	.401	.399	.397	.359	.366	.371	.410	.388
	18.15	.455	.459	.459	.467	.420	.430	.429	.426	.415	.424	.425	.474	.440
.80	-.10	.351	.352	.355	.346	.342	.333	.333	.340	.348	.352	.352	.356	.347
	6.04	.360	.360	.360	.356	.391	.419	.412	.417	.382	.388	.393	.360	.383
	12.17	.416	.416	.416	.416	.413	.440	.436	.437	.400	.407	.407	.420	.419
	18.25	.463	.464	.466	.474	.452	.467	.467	.466	.443	.449	.449	.478	.462
1.00	.27	.469	.467	.472	.471	.464	.472	.498	.497	.501	.500	.540	.569	.470
	6.40	.498	.497	.501	.500	.540	.569	.565	.568	.536	.538	.550	.498	.530
	12.58	.583	.581	.582	.581	.582	.606	.601	.605	.579	.582	.586	.584	.588
	18.76	.649	.652	.652	.656	.645	.651	.658	.642	.645	.641	.649	.649	.649
1.30	.15	.393	.393	.396	.391	.392	.392	.394	.394	.392	.392	.395	.396	.393
	6.26	.404	.405	.408	.406	.371	.406	.407	.406	.368	.369	.375	.411	.395
	12.48	.426	.424	.427	.429	.406	.425	.417	.426	.411	.407	.418	.433	.421
	18.55	.459	.455	.459	.460	.443	.456	.452	.452	.452	.448	.456	.462	.455
1.60	0	.300	.293	.300	.299	.278	.299	.296	.299	.298	.288	.299	.301	.296
	6.09	.307	.305	.309	.307	.289	.296	.293	.298	.293	.294	.294	.307	.299
	12.24	.331	.324	.331	.331	.305	.323	.307	.323	.318	.308	.322	.331	.321
	18.33	.369	.353	.366	.365	.338	.363	.352	.362	.362	.343	.365	.366	.359
2.20	.69	.131	[a].093	.128	.132	.072	.135	.129	.132	.132	[a].088	.134	.130	.126
	6.73	.165	[a].132	.161	.163	.103	.162	.161	.161	.161	[a].124	.163	.163	.156
	12.85	.178	[a].154	.178	.178	.124	.176	.173	.176	.176	[a].146	.175	.178	.171
	18.90	.198	[a].173	.195	.197	.144	.194	.189	.194	.194	[a].166	.196	.195	.190

[a]Value not used in computing average C_p.

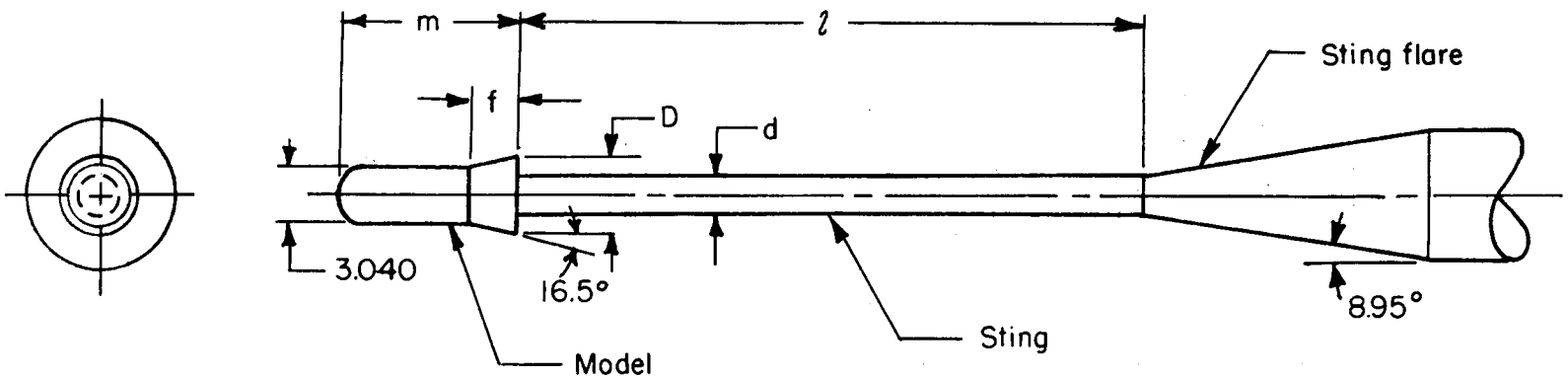

All dimensions in inches

Config.	d	l	D	d/D	l/D	f	m
1	1.125	21.3	4.435	0.254	4.80	2.37	9.57
2	2.000	↓	↓	0.451	↓	↓	↓
3	2.625	↓	↓	0.592	↓	↓	↓
4	2.00	16.3	4.435	0.451	3.68	2.37	9.57
5	↓	11.3	↓	↓	2.55	↓	↓
6	1.125	21.3	4.941	0.228	4.31	3.21	10.42
7	2.000	↓	↓	0.405	↓	↓	↓
8	2.625	↓	↓	0.531	↓	↓	↓

Figure 1.- Dimensions of model and model support.

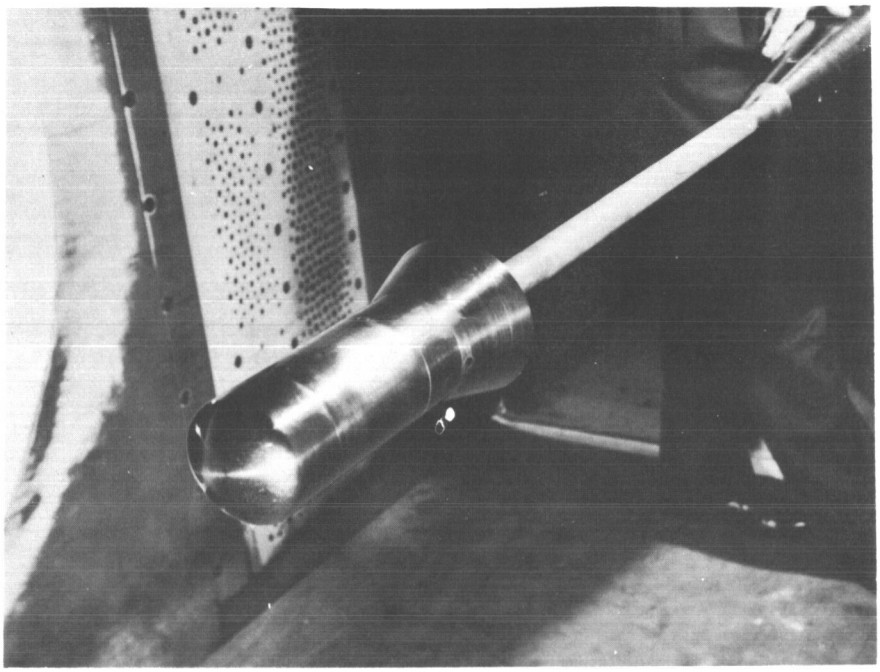

A-24400

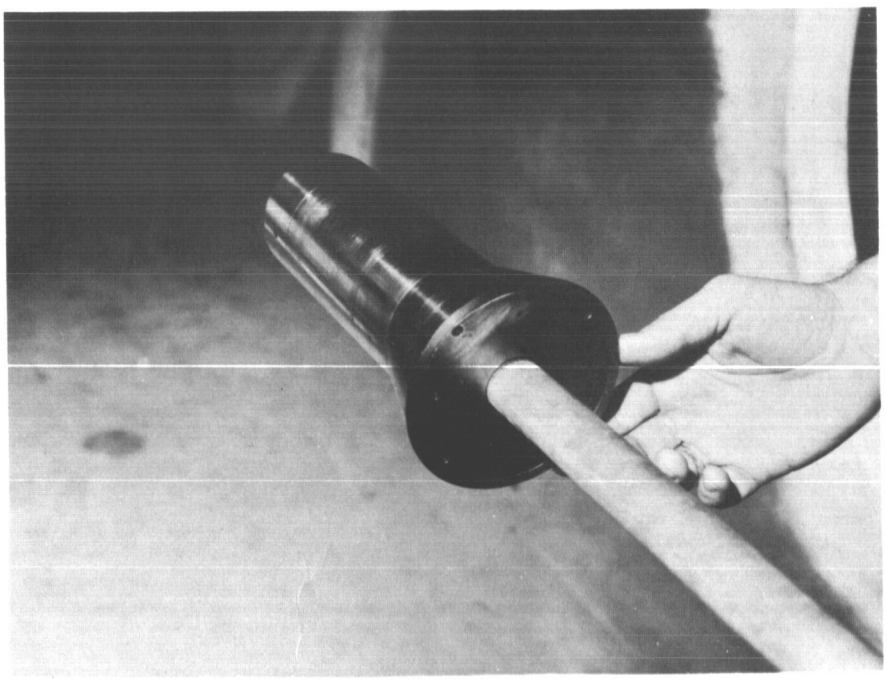

A-24401

Figure 2.- Photographs of model.

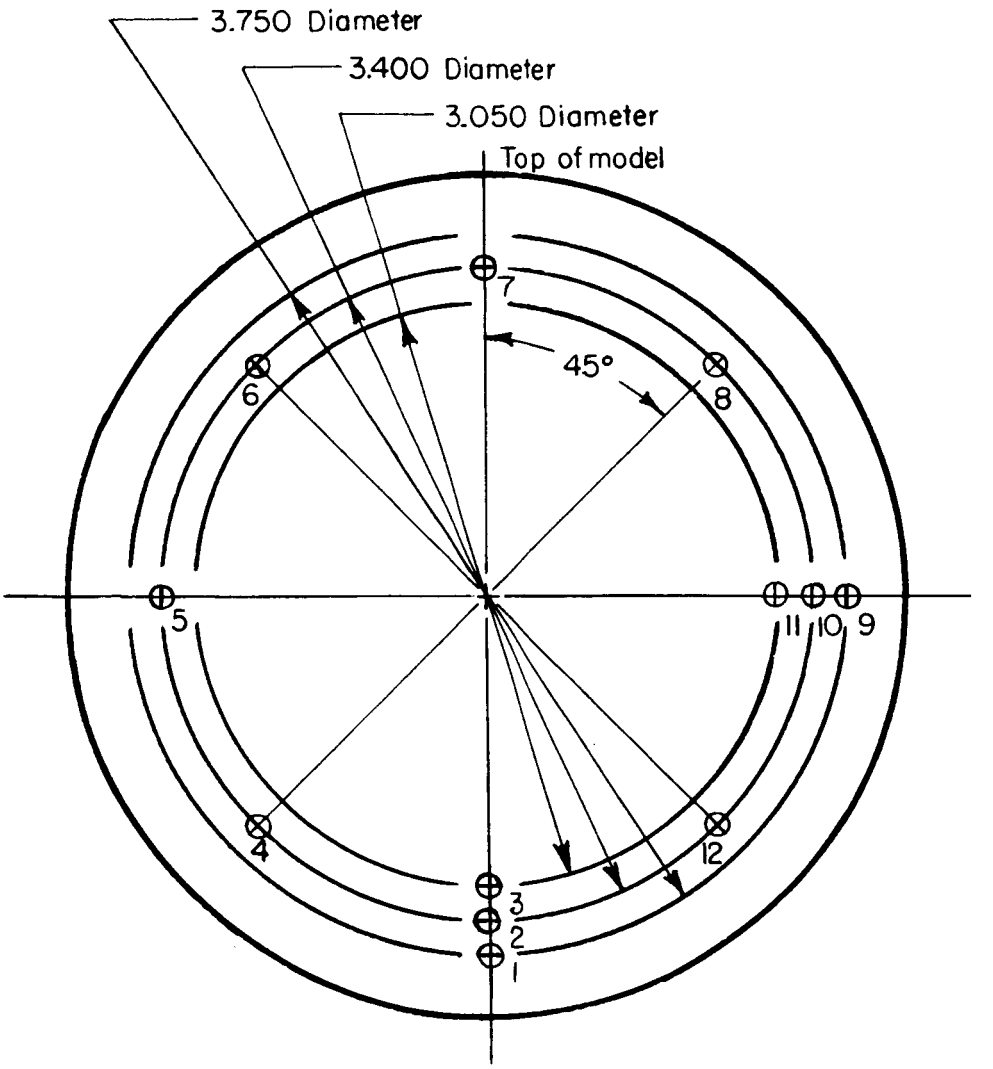

Figure 3.- Base pressure orifice location.

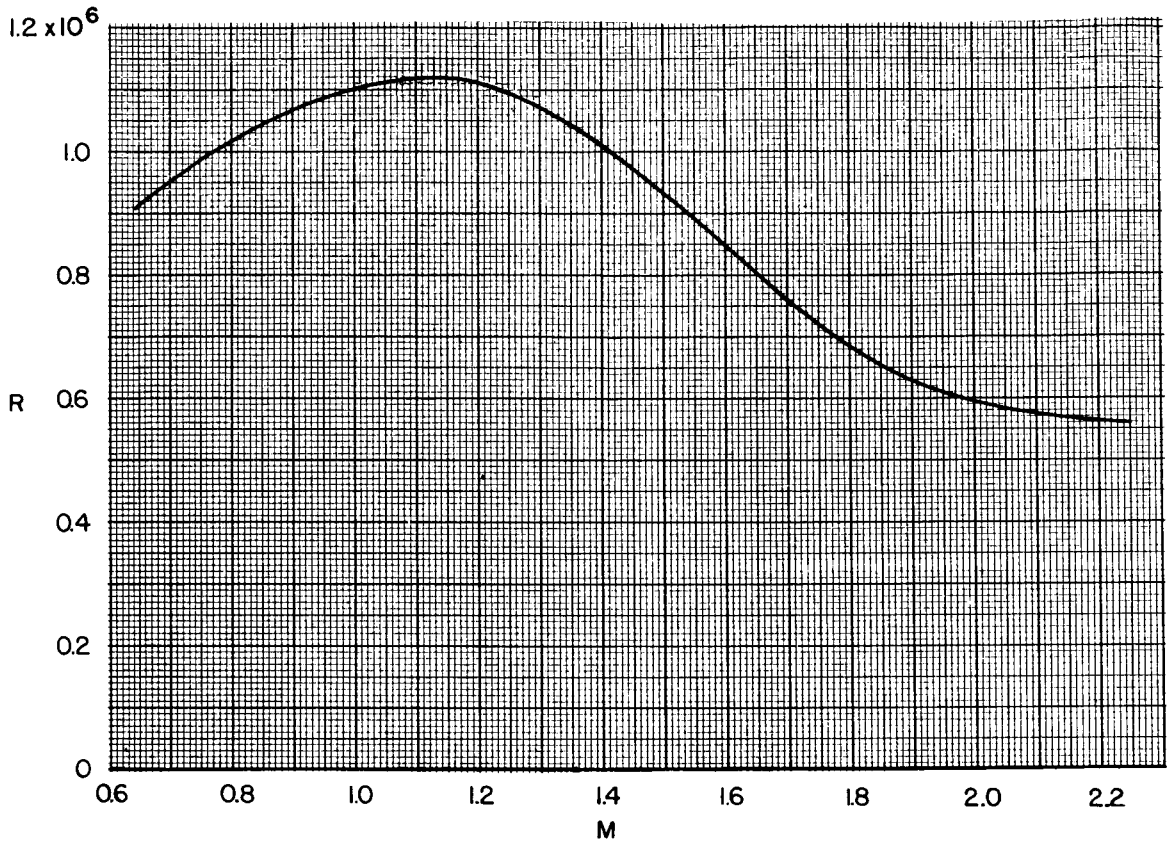

Figure 4.- Variation of Reynolds number with Mach number.

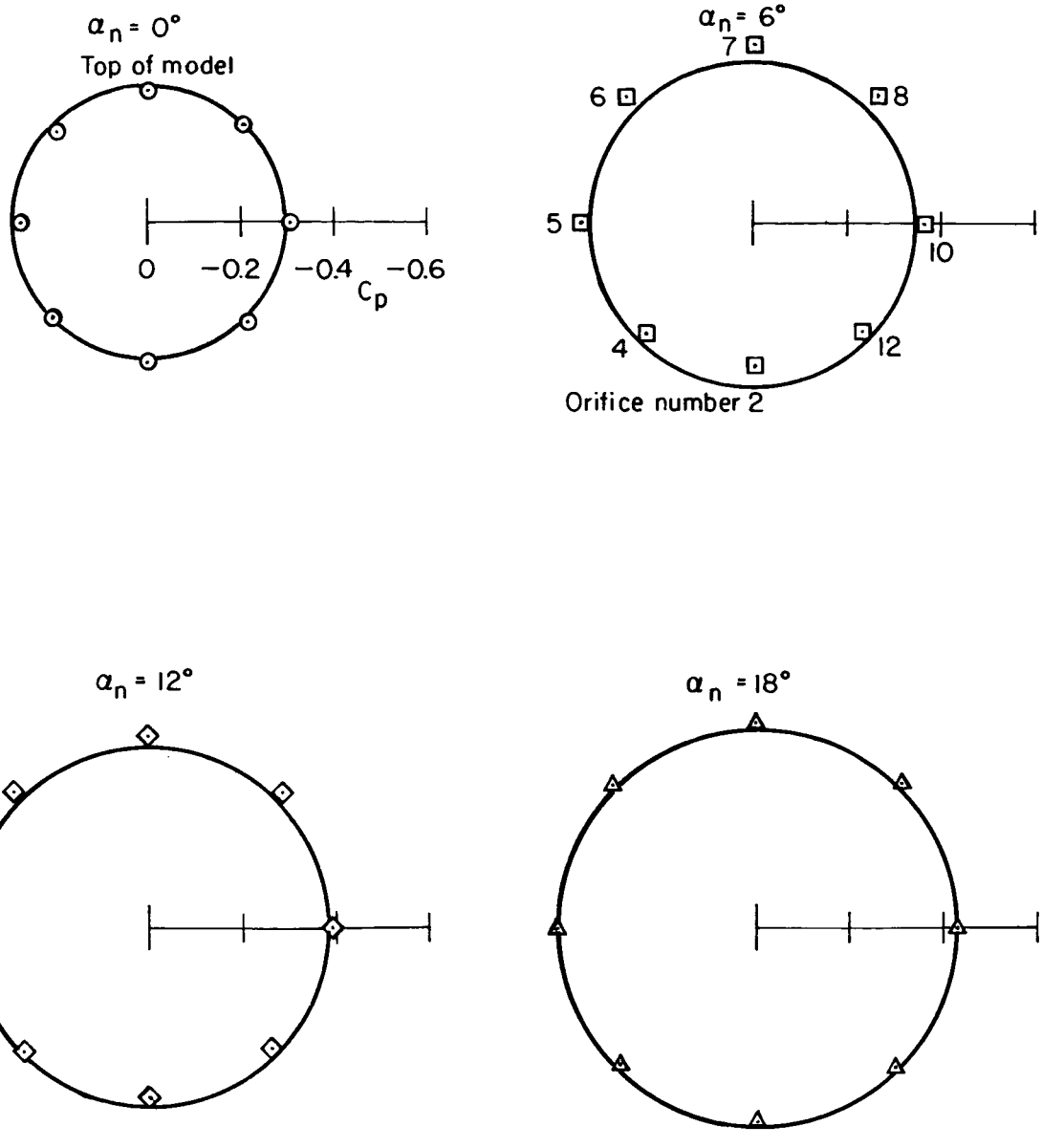

(a) M = 0.65

Figure 5.- Distribution of base pressure coefficient over model base; configuration 1.

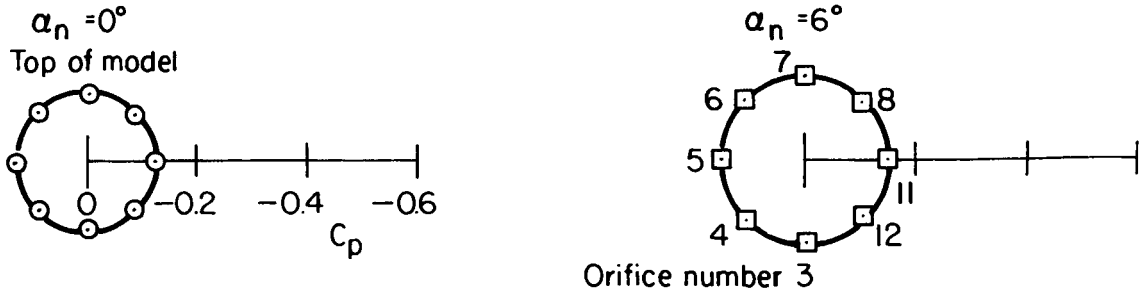

(b) M = 2.20

Figure 5.- Concluded.

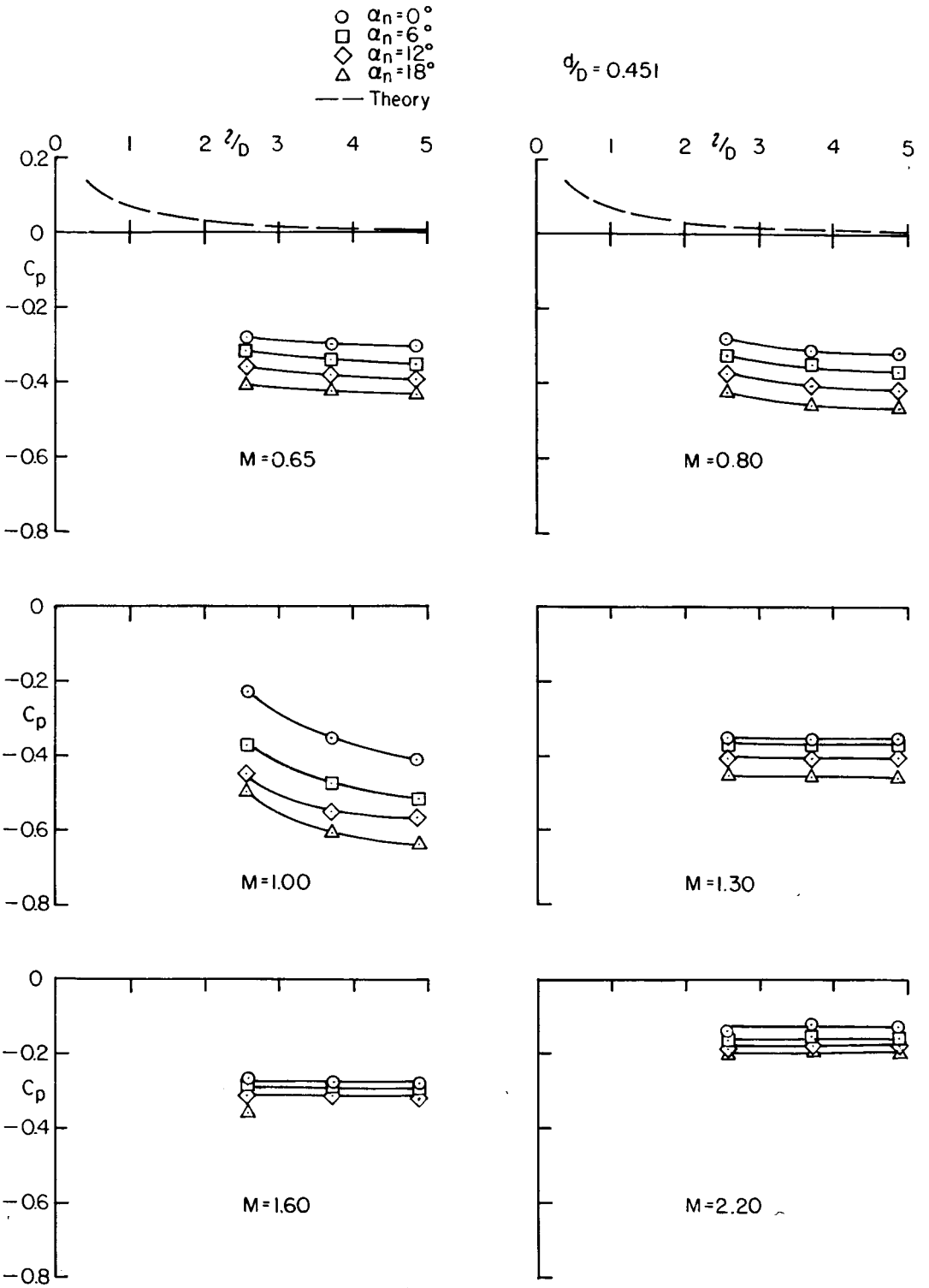

Figure 6.- Base pressure coefficient versus sting length to body base diameter ratio.

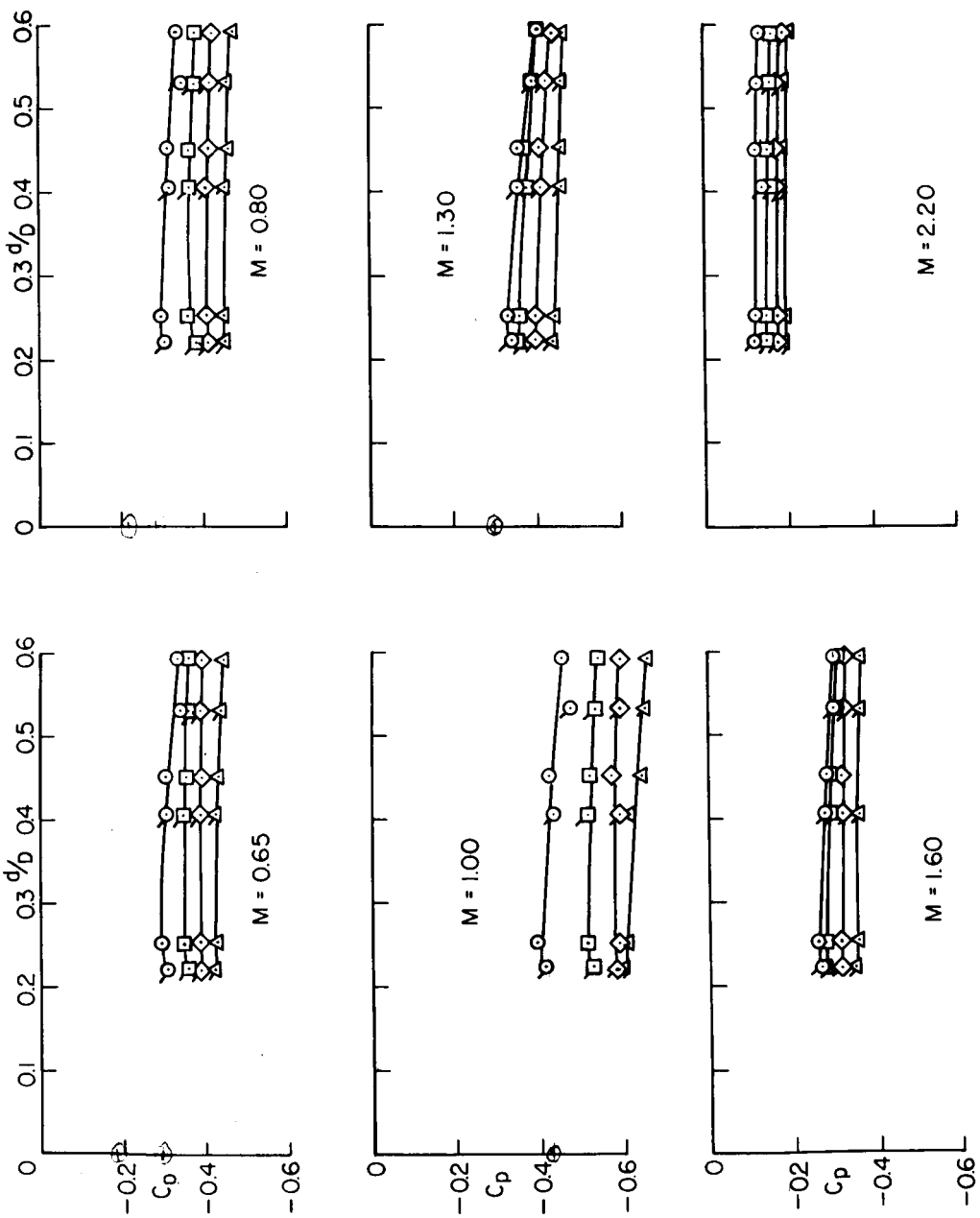

Figure 7.- Base pressure coefficient versus sting diameter to body base diameter ratio.